Sensitivity Analysis and Robust Experimental Design of a Signal Transduction Pathway System

HONG YUE,[1,4] MARTIN BROWN,[2] FEI HE,[2] JIANFANG JIA,[3] DOUGLAS B. KELL[4]

[1]*Department of Electronic and Electrical Engineering, University of Strathclyde, Glasgow* G1 1QD, UK

[2]*School of Electrical and Electronic Engineering, University of Manchester, Manchester* M60 1QD, UK

[3]*Department of Automation, North University of China, Taiyuan* 030051, *People's Republic of China*

[4]*School of Chemistry and Manchester Interdisciplinary Biocentre, University of Manchester,* 131 *Princess St., Manchester* M1 7ND, UK

Received 29 October 2007; revised 2 April 2008, 20 April 2008; accepted 20 April 2008

DOI 10.1002/kin.20369
Published online in Wiley InterScience (www.interscience.wiley.com).

ABSTRACT: Experimental design for cellular networks based on sensitivity analysis is studied in this work. Both optimal and robust experimental design strategies are developed for the IκB-NF-κB signal transduction model. Based on local sensitivity analysis, the initial IKK intensity is calculated using an optimal experimental design process, and several scalarization measures of the Fisher information matrix are compared. Global sensitivity analysis and robust experimental design techniques are then developed to consider parametric uncertainties in the model. The modified Morris method is employed in global sensitivity analysis, and a semidefinite programming method is exploited to implement the robust experimental design for the problem of measurement set selection. The parametric impacts on the oscillatory behavior of NF-κB in the nucleus are also discussed. © 2008 Wiley Periodicals, Inc. Int J Chem Kinet 40: 730–741, 2008

INTRODUCTION

Sensitivity analysis is used to understand how a model's output depends on variations in parameter values or initial conditions, and is perhaps best known in metabolic systems biology via metabolic control analysis [1–4]. It is particularly useful for complex biological networks that involve a large number of variables and parameters in which it is crucial to identify either the most important or the least relevant parameters.

Correspondence to: Hong Yue; e-mail: hong.yue@eee.strath.ac.uk.

Contract grant sponsor: National Natural Science Foundation of China.
Contract grant number: 30770560.
Contract grant sponsor: UK Biotechnology and Biological Sciences Research Council.
Contract grant number: BB/C007158/1.
Contract grant sponsor: Hong Kong Research Grants Council (to Fei He).
Contract grant numbers: CityU SRG 7001821 and CityU 122305.

Based on the nominal parameter values, local sensitivity analysis (LSA) measures the effects that small changes in the parameters have on the output. It is widely used in modeling and analysis of biological systems, in which the nominal parameter values are estimated using experimental data or computation [4–7]. For continuous dynamic systems, the local sensitivities are defined as the first-order partial derivatives of the system output with respect to the input parameters. Such information reveals the gradient of a mathematical model's output in parameter space at a given set of parameter values, and therefore plays a central role in many system identification problems.

LSA has a wide spectrum of applications in systems biology. However, for a complex and/or uncertain model in which some parameter estimates are most likely far from the true values, or for a significantly nonlinear and interactive system, it is more relevant to study global sensitivities. Global sensitivity analysis (GSA) examines the effects of simultaneous "arbitrary" variations of multiple parameters on the dependent variables under conditions in which the variations are not local [8–10]. There are different ways to perform GSA, such as screening techniques, variance-based methods, Monte Carlo filtering approaches and regression methods, and so on. In principle, GSA is valid in a bounded region around the nominal value for each parameter, and the effect of each parameter is either aggregated [11] or some worst case measures are taken for evaluation. It is not simply the result from weighted local sensitivities, but a multidimensional averaging over the whole parameter space, since when one parameter is evaluated over its interval, all the other parameters are also varying instead of keeping their nominal values. It, therefore, reveals interactions between parameters from simultaneous parameter variations. GSA has been applied in modeling, analysis, and experimental design for a range of biological systems [12–16].

Optimal experimental design (OED) is one of the techniques developed from local sensitivities, whose purpose is to devise the necessary dynamic experiments in such a way that the parameters are estimated from the resulting experimental data with the best possible statistical quality. The tasks of experimental design include input signal design, sampling rate optimization, measurement set selection, and so on. Under the assumption of uncorrelated measurement noise with zero-mean Gaussian distribution, the information content of measurements can be quantified by the Fisher information matrix (FIM) [17,18]. In general, the smaller the joint confidence interval is for the estimated parameters, the more information is contained in the measurements. In many recent works on modeling of biochemical networks, the FIM was used to design the experiments to optimize the quality of parameter estimation in a certain statistical sense [18–23]. Several strategies for solving OED problems in the context of parameter estimation for biochemical models are discussed in [24].

The quality of optimal experimental design is dependent on the accuracy of the mathematical models. The true model parameters are in most cases rarely known, and nominal or estimated parameter values are used instead. These nominal parameters may be obtained from preliminary experiments, the literature, or from previous parameter estimation. When the quality of nominal parameters is poor, the experimental design results may be overoptimistic or even misleading. In inverse modeling of complex biochemical networks, the normal way to surmount this problem is to go through an iterative/sequential process for parameter estimation and experimental design. In each iteration, the OED is implemented to provide "rich" information for a better parameter estimation in the subsequent iteration [19,25]. Using this approach, the costs associated with experiments for several iterations are nontrivial, especially for the expensive and time-consuming data collection in cellular experiments. An alternative method is the minimax experimental design, which makes the OED at the worst case in a region around the nominal parameter values. However, for a nonlinear model with a large amount of parameters, identifying the worst case for optimization of the FIM can be computationally challenging and impractical.

In this work, the problem of experimental design based on local sensitivities is addressed for biochemical systems with particular interest in models with parametric uncertainties. An optimal design on the input activation intensity is studied first using the FIM, so as to illustrate the principle of optimal experimental design. The endeavors are then focused on the robust experimental design and global sensitivity analysis, so as to take into account model uncertainties. With the results given by local and global sensitivity analyses, the influence of some important parameters on the oscillatory behavior of NF-κB in the nucleus is investigated.

LOCAL SENSITIVITIES AND OPTIMAL EXPERIMENTAL DESIGN

System Model: An Example of IκB-NF-κB Signal Pathway

For a biochemical model with n reaction species and m parameters, denote $X = [x_1 \quad x_2 \quad \cdots \quad x_n]^T$ as the state vector, $\theta = [k_1 \quad k_2 \quad \cdots \quad k_m]^T$ as the vector of

parameters. The system model can be represented by ordinary differential equations (ODEs) as

$$\dot{X} = f(X, \theta, t), \quad X(t_0) = X_0$$
$$Y = g(X, \theta, t) + \omega \tag{1}$$

where $f(\cdot)$ is the nonlinear state transition function, X_0 is the initial states vector at t_0, $g(\cdot)$ is the measurement function, $Y \in \mathbb{R}^q$ is the measurement output vector, and ω is assumed to be a zero-mean, Gaussian noise vector. There are two important assumptions for using ODEs to represent a cellular system. First, the system is assumed to be a homogeneous "well-stirred" reaction system and thus spatial distributions within each compartment are not considered, otherwise partial differential equations should be used [26]. Second, the reaction variables (molecular concentrations) are continuous functions of time. This is valid only if the number of molecules of each species in the reaction volume is sufficiently large, otherwise the discrete nature of molecules cannot be neglected and stochastic differential equations or discrete stochastic models are more appropriate [27].

The system under investigation is the NF-κB signaling pathway. The NF-κB proteins regulate numerous genes that play important roles in inter- and intracellular signaling, cellular stress responses, cell growth, survival, and apoptosis. As such, its specificity and its role in the temporal control of gene expression are of crucial physiological interest.

Models of the mainly downstream elements of an IκB-NF-κB signal pathway have been described by Hoffmann et al. [28], Nelson et al. [29], and Lipniacki et al. [30]. While Hoffmann's model measures the behavior of cell populations [28], Nelson's work analyses experimental data obtained from individual cells [29], and Lipniacki's model focuses on the role of A20, which is regulated by NF-κB and acts as an inhibitor of IKK [30]. The model used in this work is the Hoffmann's model, as described in [28,31–33]. It includes 26 reaction species participating in 64 reactions, out of which the concentrations of 24 species are time varying and are defined as state variables in the model. See Table I for the states definition. The reactions and the parameter values can be found in our previous paper [33].

Table I IκB-NF-κB Reaction Species and States

Species, States	Species, States
IκBα, x_1	IKKIκBε-NF-κB, x_{14}
NF-κB, x_2	NF-κB$_n$, x_{15}
IκBα-NF-κB, x_3	IκBα$_n$, x_{16}
IκBβ, x_4	IκBα$_n$-NF-κB$_n$, X_{17}
IκBβ-NF-κB, x_5	IκBβ$_n$, x_{18}
IκBε, x_6	IκBβ$_n$-NF-κB$_n$, x_{19}
IκBε-NF-κB, x_7	IκBε$_n$, x_{20}
IKKIκBα, x_8	IκBε$_n$-NF-κB$_n$, x_{21}
IKKIκBα-NF-κB, x_9	Source ($S = 1$)
IKK, x_{10}	IκBα$_{-t}$, x_{22}
IKKIκBβ, x_{11}	Sink (sink = 0)
IKKIκBβ-NF-κB, x_{12}	IκBβ$_{-t}$, x_{23}
IKKIκBε, x_{13}	IκBε$_{-t}$, x_{24}

Local Sensitivity Analysis and Optimal Experimental Design

Under standard assumptions, parameter estimation is obtained by solving the following optimization problem:

$$\hat{\theta} = \arg\min_{\theta} \sum_{i=1}^{q} \sum_{l=1}^{N} (y_i(\theta, t_l) - \tilde{y}_i(t_l))^T \times W_l (y_i(\theta, t_l) - \tilde{y}_i(t_l)) \tag{2}$$

where $y_i(\theta, t_l)$ and $\tilde{y}_i(t_l)$ are model predictions and measured values of the ith measurable state at time t, $(l = 1, \ldots, N)$. W_l is a square matrix with specified weighting coefficients, which is often chosen as the inverse of the measurement error covariance matrix Q, that is, $W_l = Q^{-1}$. Here, measurement errors with constant variances are considered and under the assumptions that the errors are additive, zero-mean Gaussian processes, $\hat{\theta}$ is the optimal, unbiased estimator.

At time t, the local sensitivity coefficient $s_{i,j}$ is defined as the partial derivative of the ith state to the jth parameter:

$$s_{i,j}(t) = \frac{\partial x_i(t)}{\partial \theta_j} = \frac{x_i(\theta_j + \Delta\theta_j, t) - x_i(\theta_j, t)}{\Delta\theta_j} \tag{3}$$

The sensitivity matrix $S = \partial X / \partial \theta$ is composed of elements of $s_{i,j}$ for $i = 1, \ldots, n$ and $j = 1, \ldots, m$. The sensitivity matrix is calculated using the direct differential method (DDM) where the column sensitivity vector $S_j = \partial X / \partial \theta_j$ with respect to the jth parameter (θ_j) and the system states are obtained simultaneously by solving the joint state and sensitivity profiles:

$$\begin{cases} \dot{X} = f(X, \theta, t), & X(t_0) = X_0 \\ \dot{S}_j = J \cdot S_j + F_j, & S_j(t_0) = 0 \end{cases} \tag{4}$$

where $J = \partial f / \partial X$ is the Jacobian matrix and $F_j = \partial f / \partial \theta_j$ is the parametric Jacobian matrix.

The FIM is a function of the local sensitivity matrix:

$$\text{FIM} = \sum_{l=1}^{N} S(t_l)^T Q^{-1} S(t_l) \tag{5}$$

It is an approximation of the inverse of the parameter estimation error covariance matrix (Σ), that is, $\Sigma = \text{FIM}^{-1}$. The lower bound of the variance for the ith identifiable parameter is given by $\sigma_i^2 \geq (\text{FIM}^{-1})_{ii}$. The 95% confidence interval (CI) for the ith parameter is represented as $\text{CI} = \hat{\theta}_i \pm 1.96\sigma_i$.

The covariance matrix Σ is a measure of attainable parameter estimation errors for a given set of data/experimental conditions and therefore is used as a basis for optimal experimental design. The performance index in optimal experimental design is normally a scalar function of FIM, or equivalently, a function of the error covariance matrix Σ, and it should be noted that the design depends on the estimated/nominal parameter values. Some commonly used optimal, scalarization criteria for experimental design are as follows:

$$\text{A-optimal} : \max\{\text{trace(FIM)}\} \text{ or } \min\{\text{trace}(\Sigma)\}$$

$$\text{D-optimal} : \max\{\det(\text{FIM})\} \text{ or } \min\{\det(\Sigma)\}$$

$$\text{E-optimal} : \max\{\lambda_{\min}(\text{FIM}(\theta))\} \text{ or } \min\{\lambda_{\max}(\Sigma)\}$$

$$\text{Modified E-optimal} : \min\left\{\frac{\lambda_{\max}(\text{FIM})}{\lambda_{\min}(\text{FIM})}\right\}$$

where $\lambda_{\min}$ and $\lambda_{\max}$ are the minimum and the maximum eigenvalues and det indicates the determinant of a matrix. The A-optimal design minimizes the trace of the covariance matrix (sum of eigenvalues). However, this criterion is rarely used since it can lead to noninformative experiments when Σ is not positive definite [34]. The D-optimal design minimizes the determinant of the covariance matrix (product of eigenvalues) and can thus be interpreted as minimizing the geometric mean of the errors in the parameters. The largest error is minimized by the E-optimal design, which corresponds to a minimization of the largest eigenvalue of Σ. The modified E-optimal design minimizes the ratio of the largest to the smallest eigenvector and thus optimizes the functional shape of the confidence intervals. The relationship between these various criteria has been well studied [35]. Note that all these scalarization criteria result in a convex optimization problem when the FIM is a linear function of the experimental design parameters.

Optimal Experimental Design of IKK Activation Level

To illustrate the principle of optimal experimental design for the IκB-NF-κB signal pathway, the problem of selecting the IKK activation intensity using dynamic (local) sensitivity analysis will be addressed. The FIM is used along with the Cramer–Rao theorem to determine the optimal step input signal so that the estimated parameters have a minimum variance. Taking IKK as the step input and nuclear NF-κB (x_{15}) as the system output, the previously described four criteria are applied in the design and the results are compared.

To make a better illustration, only three parameters (k_9, k_{28}, and k_{36}) are estimated in the example. These three parameters are all identified to be influential in our previous study of LSA [31,33]. The range of the initial IKK concentration after equilibration is set to [0.01, 1] μM. The simulation shows that the optimal IKK input intensity is 0.06 μM with the A-, D-, and E-optimal designs, and it is 0.01 μM for the modified E-optimal design. The 95% parameter confidence intervals for these two results are given in Fig. 1. It can be clearly seen that while the parametric uncertainty region for the E-optimal design has a smaller volume for all parameters, the modified E-optimal design produces a more circular uncertainty region. The corresponding 95% confidence intervals for each pair of parameters and their percentage estimation errors are listed in Table II, for the E-optimal and the modified E-optimal design. The results in Fig. l and those in Table II are consistent.

The above design shows that the optimal experimental design is quite straightforward to be implemented once the local sensitivity matrices are established. Different optimization criteria can be employed to determine the best experimental conditions for parameter estimation. Results from different criteria may sometimes be different since these criteria represent scalarized measures of the covariance matrix. Consequently, preference information about the parameter importance may be used to rank the different solutions. It can be clearly seen that the OED results depend on the quality of the model/sensitivity used and the results can be poor when the model uncertainty cannot be ignored. In this case, robust strategies need to be developed for the experimental design.

ROBUST EXPERIMENTAL DESIGN OF MEASUREMENT SET SELECTION

The objective of robust experimental design (RED) is to optimally design experiments when there exists model uncertainty. As with OED, the aim is to design the experiments so that the uncertainties in the estimated parameters are as small as possible. However, when the sensitivity matrix, and hence the FIM, is a function of the parameters, the design results will

Table II Ninety-five Percent Confidence Intervals and Estimation Errors

Parameters		E-Optimal Design		Modified E-Optimal Design	
		95% CI	Error%	95% CI	Error%
(k_9, k_{28})	$\hat{k}_9$	[0.02002, 0.02078]	1.87	[0.01491, 0.02589]	26.93
	$\hat{k}_{28}$	[0.01507, 0.01793]	8.65	[0.01169, 0.02130]	29.11
(k_{28}, k_{36})	$\hat{k}_{28}$	[0.01567, 0.01732]	5.01	[0.01416, 0.01887]	14.27
	$\hat{k}_{36}$	[0.00377, 0.00439]	7.72	[0.00315, 0.00501]	22.84
(k_9, k_{36})	$\hat{k}_9$	[0.01907, 0.02173]	6.52	[0.01704, 0.02379]	16.54
	$\hat{k}_{36}$	[0.00389, 0.00428]	4.78	[0.00313, 0.00503]	23.28

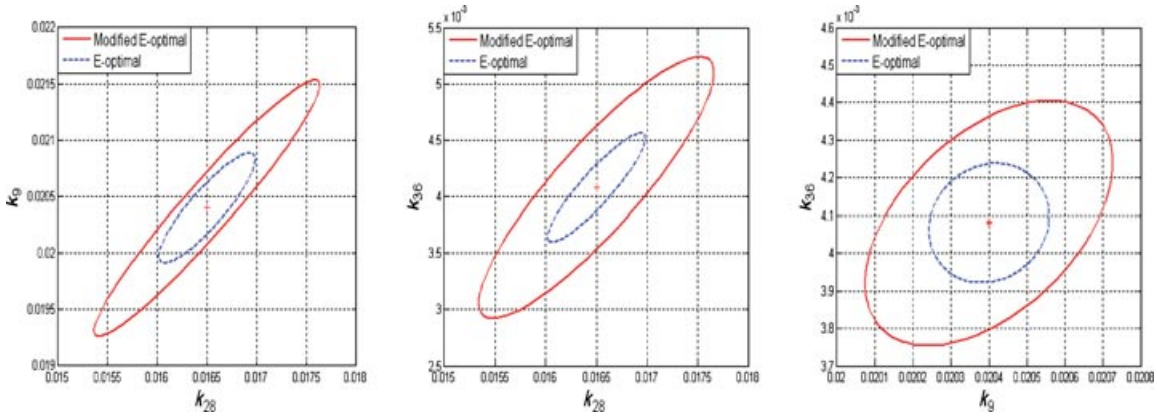

Figure 1 Confidence intervals with respect to two different IKK activation intensities calculated by the E-optimal (0.06 μM) and the modified E-optimal (0.01 μM) design. [Color figure can be viewed in the online issue, which is available at www.interscience.wiley.com.]

be biased because the parameters are unknown. Sequential experimental design strategies that repeatedly estimate the parameters and redesign the experiments could be used; however, this is expensive in terms of the number of experiments. RED is an alternative that produces an experimental design that is valid across a prespecified parameter range around the nominal values.

The problem of measurement set selection is applicable when there are a large number of states that could be measured, but experimental constraints mean that only a small number can actually be measured. This is represented as the selection problem:

$$\xi = \begin{Bmatrix} x_1 & \cdots & x_n \\ \omega_1 & \cdots & \omega_n \end{Bmatrix}, \sum_{i=1}^{n} \omega_i = 1, \omega_i \geq 0, \forall i \quad (6)$$

where ω_i is the nonnegative weight relating to the ith state x_i. The selection problem is originally an integer-programming problem as the weights should be binary variables; however, this is relaxed to produce an approximate, continuous optimization problem. RED estimates the weights and consequently focuses on those measurements with larger weight values, that is, state measurements that are more informative for parameter estimation. This is a vector optimization problem over the positive semidefinite cone, for which several scalarizations have been proposed, such as D-optimal, A-optimal, E-optimal, and so on.

Semidefinite Programming and Robust Experimental Design

Ideally the design should start from parametric uncertainties and map these uncertainty information into uncertainty bound in FIM. This mapping is difficult to be established explicitly, but the link via Taylor expansion can be managed. Considering a local model with additive uncertainties to the model parameters, the corresponding parametric sensitivity matrix can be represented by a simple truncated first-order Taylor expansion:

$$S(\theta + \Delta\theta) \approx S(\theta) + \frac{\mathrm{d}S(\theta)}{\mathrm{d}\theta}\Delta\theta \quad (7)$$

Here, only the first-order expansion is kept in the approximation. $dS/d\theta$ is the second-order parametric sensitivity and is represented by a 3D matrix (state-by-parameter-by-parameter). The FIM can then be locally expressed as

$$\begin{aligned}\mathrm{FIM}(\theta+\Delta\theta) &= S(\theta+\Delta\theta)^T Q^{-1} S(\theta+\Delta\theta)\\ &= S(\theta)^T Q^{-1} S(\theta)\\ &\quad + (\Delta\theta)^T \left(\frac{dS(\theta)}{d\theta}\right)^T Q^{-1} S(\theta)\\ &\quad + (S(\theta))^T Q^{-1} \frac{dS(\theta)}{d\theta}\Delta\theta\\ &\quad + (\Delta\theta)^T \left(\frac{dS(\theta)}{d\theta}\right)^T Q^{-1} \frac{dS(\theta)}{d\theta}\Delta\theta\end{aligned} \tag{8}$$

Assuming that the parametric uncertainty is bounded by $\|\Delta\theta\| < c$, for a some small value c (small region around the nominal parameter values), the second- and higher order terms of $\Delta\theta$ can be neglected; thus,

$$\begin{aligned}\mathrm{FIM}(\theta+\Delta\theta) &= S(\theta)^T Q^{-1} S(\theta) + (\Delta\theta)^T \left(\frac{dS(\theta)}{d\theta}\right)^T\\ &\quad \times Q^{-1} S(\theta) + (S(\theta))^T Q^{-1} \frac{dS(\theta)}{d\theta}\Delta\theta\\ &= \mathrm{FIM}(\theta) + \bar{\Delta}\end{aligned} \tag{9}$$

where $\bar{\Delta}$ can be regarded as the transformed parametric uncertainty to the additive uncertainty in FIM. For a small parametric uncertainty $\Delta\theta$, to use the FIM as a measure in a region, we could take the average value or the worst case value (smallest—least informative). To consider large uncertainties in parameters, the interpretation is to relate the assumptions on $\bar{\Delta}$ to the second and possibly higher order terms of the parametric uncertainties $\Delta\theta$.

On the basis of the understanding that the parametric uncertainty can be linked with uncertainty in FIM, we used the method proposed by Flaherty and his coauthors [36] to perform robust experimental design on the measurement set selection. The weighting matrix in FIM is taken to be $W_l = W = \mathrm{diag}[\omega_1 \quad \cdots \quad \omega_n]$ for all t_l. Consider the additive uncertainty to form an updated FIM represented by

$$\mathrm{FIM} = \sum_{i=1}^{n} \omega_i \left(S_i^T S_i + \Delta_i\right) \tag{10}$$

where Δ_i is an $m \times m$ matrix for $i = 1, \ldots, n$, S_i is the ith row of the sensitivity matrix. Denoting $\Delta = \mathrm{blkdiag}(\Delta_1, \ldots, \Delta_n)$, a spectral norm bound is given on the magnitude of the perturbations by $\|\Delta\| \le \rho$. ρ is the uncertainty bound. The robust E-optimal design can be cast as the following semidefinite program (SDP) [36,37]:

$$\begin{aligned}&\min \max \|\Delta\| \le \rho^{-s}\\ &\text{subject to } \sum_{i=1}^{n} \omega_i \left(S_i^T S_i + \Delta_i\right) \ge s\mathbf{I}_m\\ &\qquad \sum_{i=1}^{n} \omega_i = 1, \omega_i \ge 0\end{aligned} \tag{11}$$

By employing linear fractional representation and assuming that $\Delta_1 = \cdots = \Delta_n$, the SDP problem in (11) can be transferred into a regularized optimization problem [36]:

$$\begin{aligned}&\min -s\\ &\text{subject to } \sum_{i=1}^{n} \omega_i S_i^T S_i - \rho\sqrt{n}\|W\|_2 \ge s\mathbf{I}_m\end{aligned} \tag{12}$$

with the uncertainty bound ρ as the regularization parameter.

Results and Discussion on Robust Measurement Set Selection

The robust experimental design is applied to the IκB-NF-κB model to estimate which subset of measurements provides more information for parameter estimation when the system is subject to uncertainties. In the simulation study, we take $\Delta_1 = \cdots = \Delta_{24}$ and set the uncertainty range to be $\rho \in [1e-6, 10]$. The change of weights with respect to the uncertainty bound ρ can be calculated for each state. Those weights with comparatively large values are shown in Fig. 2 and the rest are shown in Fig. 3. Each weight ω_i corresponds to a state x_i. The larger the value of ω_i is, the more contribution the state x_i has to the parameter estimation. Therefore, those states with larger weight values should be considered in the measurement set selection with high priority.

In robust experimental design, when the uncertainty measure is very small, that is, when the model is close to its nominal parameters, the measurements (states) with more influential effects can be clearly distinguished from those that are less informative for parameter estimation. However, when the uncertainty is large, all the weights converge to the same value. That is to say, the difference in the contribution of different states disappears under large uncertainty. This is

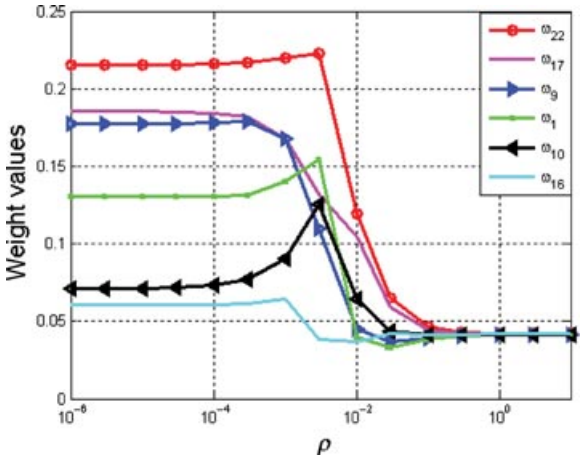

Figure 2 Change of weights with respect to ρ. These six weight variables have larger values when ρ is small compared with the rest of the weight variables. When ρ is large, all the weights have the same value of 0.417. [Color figure can be viewed in the online issue, which is available at www.interscience.wiley.com.]

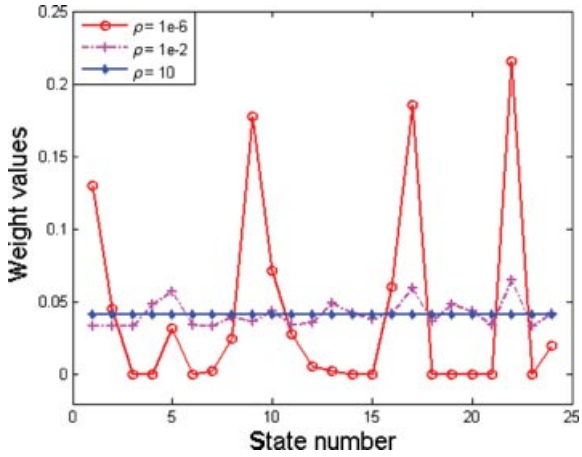

Figure 4 Distribution of weight values at three uncertainty levels, $\rho = 1e-6$ corresponds to small uncertainty, $\rho = 10$ corresponds to large uncertainty, and $\rho = 1e-2$ corresponds to the uncertainty level in between the other two. [Color figure can be viewed in the online issue, which is available at www.interscience.wiley.com.]

expected because when the knowledge about the model is poor, there is little information to choose which states are the most informative.

To further illustrate the results, the 24 weight values at three different uncertainty levels, $\rho = 1e-6$ (small uncertainty), $\rho = 1e-2$ (middle uncertainty), and $\rho = 10$ (large uncertainty), are compared in Fig. 4. It can be seen that the weights distribution in the case of $\rho = 10$ is almost uniform, whereas the weight distribution for $\rho = 1e-6$ has a large variation. The weight value distribution with middle uncertainty stays in between these two extrema. Therefore, the uncertainty measure, ρ, can be regarded as a regularization factor that trades off robustness against the number of states needed to provide satisfactory parameter estimation. It should be noted that this robust experimental design naturally reduces to optimal experimental design when $\rho = 0$.

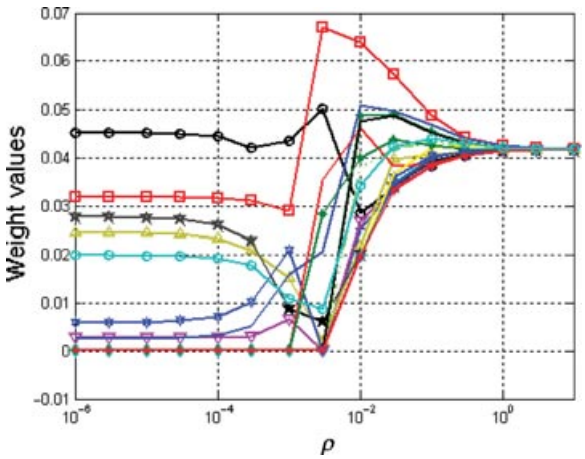

Figure 3 Change of weights with respect to ρ. These weights are $\omega_2, \omega_5, \omega_{11}, \omega_8, \omega_{24}, \omega_{12}, \omega_7, \omega_{13}, \omega_{14}, \omega_3, \omega_{18}, \omega_{20}, \omega_6, \omega_4, \omega_2, \omega_{15}, \omega_{19}, \omega_{23}$. Compared with the six weights in Fig. 2, they have smaller values when ρ is small. When ρ is large, all the weights also have the same value of 0.417. [Color figure can be viewed in the online issue, which is available at www.interscience.wiley.com.]

The robust experimental design in this work is parameterized by the model uncertainty bound ρ. This is different from the optimal experimental design that is based on FIM evaluated at the nominal parameter values. Owing to the limitation of current measurement techniques in exploring cellular networks, and also due to the fact that cellular network systems often contain a large number of parameters, large parametric uncertainties are almost unavoidable in any cell network models. It is, therefore, crucial to implement robust experimental design and to understand the impacts of parameters on system dynamics from a global point of view.

GLOBAL SENSITIVITY ANALYSIS AND OSCILLATION UNCERTAINTY

Modified Morris Method

Global sensitivity analysis investigates the parametric influence on the system output in a large region around the nominal parameter values, and as such takes into account nonlinear effects and interactions between parameters. The Morris method is used for GSA because of its computational efficiency.

The Morris method is a screening method that is based on what is called an elementary effect (EE). Through a predefined random sampling strategy, a certain number of EEs are obtained for each factor (i.e., parameter) [38]. The distribution of the EEs associated with the ith input factor is denoted as F_i. Two sensitivity measures are used for each factor: (1) μ_i, the mean of F_i, an estimate of the overall effect of the ith input factor on the output; and (2) σ_i, the standard deviation of F_i, an estimate of the ensemble of the factor's effects, due to either nonlinear and/or interactions with other factors. These two measures will be used as indicators of importance.

Consider a model for which the output y is a deterministic function of the m input factors (parameters), that is, $y = g(k_1, \ldots, k_m)$. Assuming that each parameter, k_i, is scaled in the interval [0, 1] and may take values from $\{0, 1/(p-1), 2/(p-1), \ldots, 1\}$, then the region of interest, Ω, is an m-dimensional, p-level grid. The EE of the ith input is defined as

$$EE_i(\theta) = \frac{g(k_1, k_2, \ldots, k_{i-1}, k_i + \Delta, k_{i+1}, \ldots, k_m) - g(\theta)}{\Delta} \quad (13)$$

where $\theta = [k_1 \quad \cdots \quad k_m] \in \Omega$, $k_i \leq 1 - \Delta$. Δ is a predetermined multiple of $1/(p-1)$ and is taken to be $\Delta = p/[2(p-l)]$ in this work. Producing a value for F_i requires random selection of a value for each $k_i (i = l, 2, \ldots, m)$ from the grid and evaluation of y twice, one at the selected m values, the other at the values after increasing k_i by the quantity of Δ. The difference between these two runs yields one elementary effect. This calculation will be repeated r times to produce a random sample of r EEs for each F_i. Owing to its designed sampling strategies, this method is computationally cheap as it requires a relatively small number of model evaluations.

In the original Morris method, all the input factors were assumed to be uniformly distributed in the same [0, 1] intervals. For signal transduction pathway models, parameter ranges are normally different and widely dispersed; therefore, a log-uniform distribution is preferred for the random sampling strategy. Also, different lower and upper bounds are considered for each parameter and in this paper, this is known as the modified Morris method [39].

Global Sensitivity Analysis of IκB-NF-κB Model

The modified Morris GSA method is implemented to analyze the IκB-NF-κB signal transduction pathway model, using the variable of nucleus NF-κB concentration (x_{15}). The number of measures for each input factor is taken to be $r = 100$, the grid level is $p = 10$, and the simulation length is 400 min. Simulations are carried out for two cases: one is focused on a local range, which is ±5% around the nominal value θ_0 (Fig. 5); the other is in a wide range of two orders variations on both sides of θ_0, that is, [0.01 θ_0, 100 θ_0] (Fig. 6).

A number of observations have been obtained from the Morris GSA:

(a) When the GSA is implemented within a narrow range around the nominal parameter values, the sensitivity ranking results from GSA using the modified Morris method agrees well with the results from LSA shown in our previous work

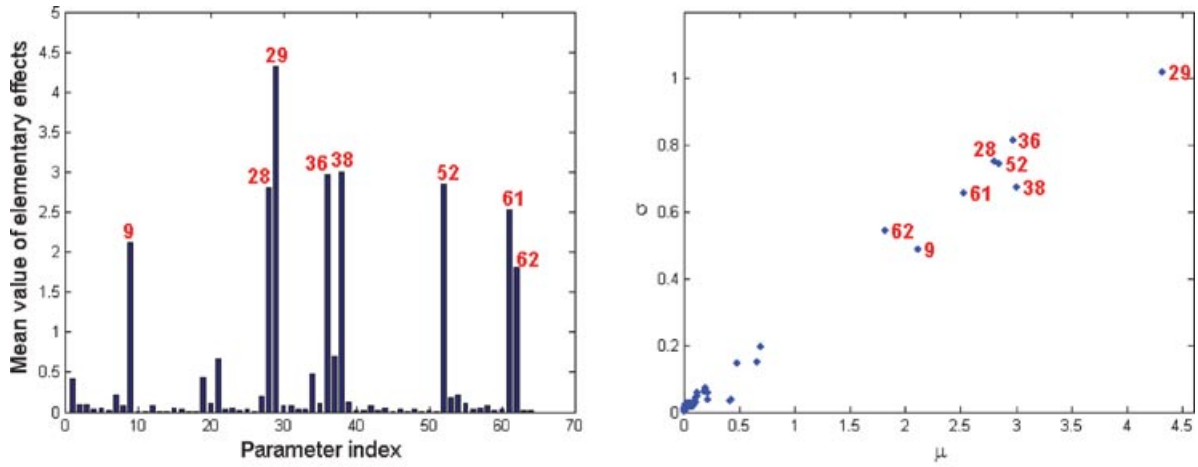

(a) Mean values of EEs (b) (μ–σ) plane by GSA

Figure 5 Morris sensitivity analysis within a narrow range [0.95, 1.05] θ_0. [Color figure can be viewed in the online issue, which is available at www.interscience.wiley.com.]

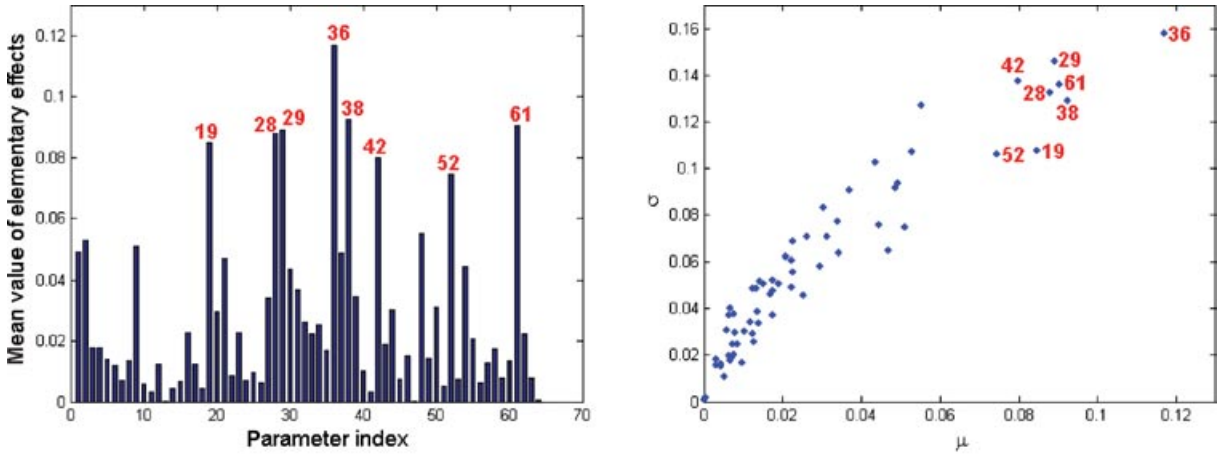

Figure 6 Morris sensitivity analysis within a large range [0.01, 100] θ_0. [Color figure can be viewed in the online issue, which is available at www.interscience.wiley.com.]

[31,33]. This is particularly true for those sensitive parameters when they are clearly distinguished from the rest set of parameters.

(b) For GSA performed in a large parameter range, different sensitive parameters are identified, for example, k_{19} and k_{42} in Fig. 6. Their effects in terms of nonlinearity and/or interactions are neglected in local analysis. In the IκB-NF-κB signal pathway system, k_{19} is the NF-κB nuclear import rate, which impacts all the reactions involving NF-κB in the nucleus and may reasonably be expected to contribute significantly to the system output. Parameter k_{42} is the constitutive IκBβ translation rate. The biological implication of its influential contribution to NF-κB in the nucleus cannot be clearly revealed by the authors unfortunately.

(c) The parameter sensitivities in GSA are more evenly distributed compared with that of LSA (see Fig. 5a and Fig. 6a). Here we use the local range GSA result to represent the LSA result since they are almost the same. The comparatively dispersed distribution of GSA is due to the fact that interactions between parameters are considered.

(d) In the $(\mu - \sigma)$ plots in Fig. 5b and Fig. 6b, a large value of μ, indicates an input factor with an important overall influence on the output. A large value of σ indicates an input whose influence is highly dependent on the values of other inputs or whose effect is highly nonlinear. It is worth noting that the relationship between μ and σ is approximately linear. This is true for most GSA using the Morris method since the majority of the models encountered in natural science are highly nonlinear [40]. Thus, a factor that is important in the model is usually more involved in curvature or interactive effects and vice versa. The slope of the relationship is not necessarily relevant in the study of GSA.

Impacts of Sensitive Parameters on Oscillation Behavior

Since the oscillation of NF-κB$_n$ is an important feature of this signal transduction pathway [25,29], it is crucial to understand how the variation of sensitive parameters affects its oscillation patterns. Based on both LSA and GSA results, k_{36}, k_{28}, and k_{61} have been chosen as the sensitive parameters to study the impacts of their variations on the oscillation of NF-κB$_n$. Only one parameter is changed in each run, and the value is taken as the nominal value multiplied by a factor γ. In Figs. 7–9a, the initial conditions of IKK after equilibrium are set to be 0.1 μM. The uncertainty range of k_{36} in which damped oscillations can be practically observed is roughly one order around the nominal value, whereas for k_{28} the uncertainty range that produces damped oscillations is much larger. Within these uncertainty ranges, the amplitude and phase of oscillation change a lot. The observation of the parameter range in which oscillations occur at all is particularly important for parameter estimation as it straightforwardly reduces the search space for uncertain parameters.

When focusing on another sensitive parameter, the IKK decay rate k_{61}, extra insights about the oscillation of NF-κB$_n$ can be discovered. Figure 9a shows that when k_{61} is varied from 0 to 4 times of its nominal value, the NF-κB$_n$ profile goes through several damped oscillations until it reaches the steady state

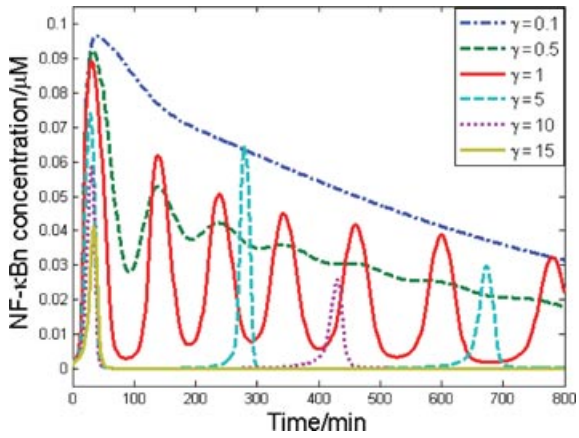

Figure 7 NF-κB$_n$ oscillation with respect to variations in k_{36}. [Color figure can be viewed in the online issue, which is available at www.interscience.wiley.com.]

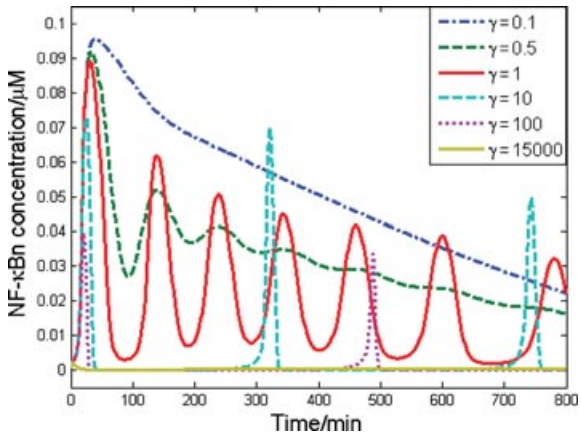

Figure 8 NF-κB$_n$ oscillation with respect to variations in k_{28}. [Color figure can be viewed in the online issue, which is available at www.interscience.wiley.com.]

without oscillation. This is under the condition that the initial concentration of IKK after equilibrium is kept to be 0.1 μM. However, when this initial condition is set to be 0.03 μM, a sustained oscillation of NF-κB$_n$ is obtained when $k_{61} = 0$ (as shown in Fig. 9b). This means that a constant activation level of IKK can produce sustained oscillations of NF-κB in the nucleus when the activation level is kept within a certain range. Similar scenarios can be found in a simulation study of inhibitor drug effects on the dynamics of NF-κB signal pathway by Sung and Simon [41]. In their work, they introduced molecules with different inhibitory targets. It was observed that when the drug dosage is controlled at certain levels, IKK is constitutively active and the nuclear NF-κB exhibits sustained oscillations (see Fig. 4a in [41]). Although the biophysical feasibility of this scenario in NF-κB pathway is not clear yet, with the help of nonlinear dynamic analysis, for example, bifurcation analysis, the conditions under which sustained oscillations of nuclear NF-κB will occur can be identified.

Robust analysis of the sensitive parameters is important for cell networks with oscillation behavior. This is also revealed by some studies of other oscillation networks. An example is the study of cyclic monophosphate (cAMP) oscillations, which shows that a small but significant portion of uncertain parameters can seriously affect the sustained oscillations [42].

CONCLUSIONS

In this work, optimal and robust experimental design procedures are discussed for the IκB-NF-κB signal pathway model, using local and global parametric sensitivity analysis. Initially, a local, optimal experimental

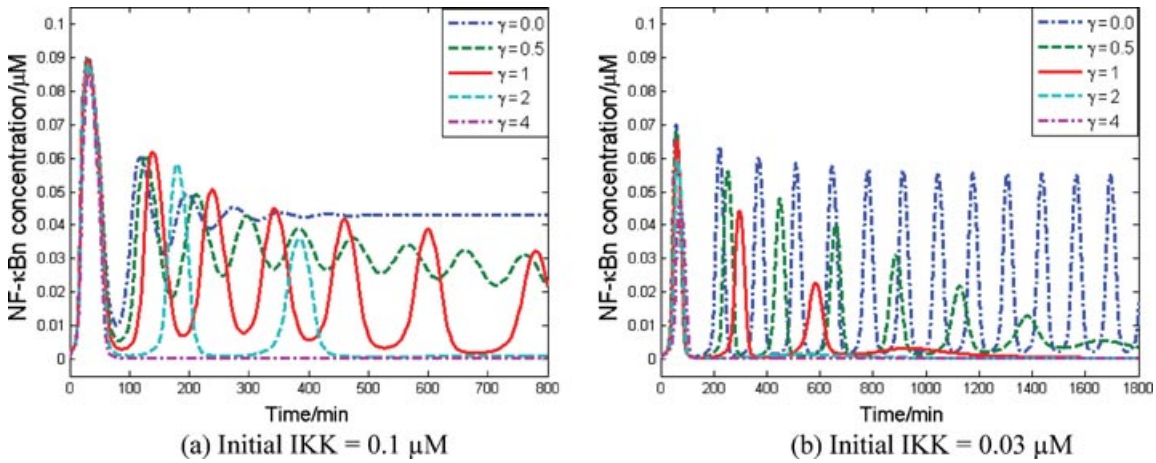

Figure 9 NF-κB$_n$ oscillations with respect to variations in k_{61}. [Color figure can be viewed in the online issue, which is available at www.interscience.wiley.com.]

design is used to determine the starting IKK activation intensity as part of a simplified three parameter estimation problem. It is shown that in this simple scenario, the A-, D-, and E-optimal designs produce similar results as they all chose the same IKK activation intensity that minimized the parametric uncertainty in estimation. However, using local techniques such as these are only approximately valid because the measure of parametric uncertainty, the FIM, depends on the optimal parameters which are, of course, unknown. A number of robust experimental design methods have been developed to address this problem, and this paper described a RED with the minimax design principle, in which it is assumed that the parameters lie within a bounded region around the nominal values. It is interesting to compare this minimax robust experimental design with the Morris GSA as both methods are based on the assumption of bounded and known parametric uncertainties. In the RED method, the performance function is optimized at the worst case (largest norm of uncertainty factor), which turns out to be a minimax robust design. In the Morris GSA, the sensitivity measure, which is the elementary effect, is evaluated at a number of sampling points and the "averaged" result is used to represent the global sensitivities. While in the minimax RED, the nominal local model is used with uncertainty bound considered, in the Morris GSA, there is no such a nominal model because in each calculation, the base parameter vector is randomly chosen from the parameter domain. The idea of Morris GSA can be used to develop another group of robust experimental design methods, which uses "averaged" information on FIM instead of the current minimax design. The work along this line is under investigation.

Based on the sensitivity analysis, the study is also undertaken for the parametric impacts on the oscillatory behavior of NF-κB in the nucleus. It shows that sensitivity analysis can provide information on signaling pathway systems, which are not necessarily obvious in the dynamic model itself. In particular, very small changes in certain sensitive parameters can cause significant changes to the oscillation patterns, say from damped oscillations to sustained oscillations, or vice versa.

BIBLIOGRAPHY

1. Fell, D. A. Understanding the Control of Metabolism; Portland Press: London, 1996.
2. Heinrich, R.; Schuster, S. The Regulation of Cell Systems; Chapman & Hall: New York, 1996.
3. Kell, D. B.; Westerhoff, H. FEMS Microbiol Rev 1986, 39, 305–320.
4. Ingalls, B. P.; Sauro, H. M. J Theor Biol 2003, 222, 23–36.
5. Degenring, D.; Froemel, C.; Dikta, G.; Takors, R. J Process Cont 2004, 14, 729–745.
6. Schwacke, J. H.; Voit, E. O. J Theor Biol 2005, 236, 21–38.
7. Zak, D. E.; Stelling, J.; Doyle, F. J. III. Comput Chem Eng 2005, 29, 663–673.
8. Varma, A.; Morbidelli, M.; Wu, H. Parametric Sensitivity in Chemical Systems; Cambridge University Press: Cambridge, UK, 1999.
9. Seferlis, P.; Hrymak, A. N. Comput Chem Eng 1996, 20, 1177–1200.
10. Turanyi, T. J Math Chem 1990, 5, 203–248.
11. Saltelli, A.; Tarantola, S.; Campolongo, F.; Ratto, M. Sensitivity Analysis in Practice: A Guide to Assessing Scientific Models; Wiley: New York, 2004.
12. Bentele, M.; Lavrik, I.; Ulrich, M.; Stößer, S.; Heermann, D. W.; Kalthoff, H.; Krammer, P. H.; Eils, R. J Cell Biol 2004, 166, 839–851.
13. Cho, K.-H.; Shin, S.-Y.; Kolch, W.; Wolkenhauer, O. Simulation 2003, 79, 726–739.
14. Kontoravdi, C.; Asprey, S. P.; Pistikopoulos, E. N.; Mantalaris, A. Biotechnol Prog 2005, 21, 1128–1135.
15. van Kiel, N. A. W. Briefings Bioinform 2006, 7, 364–374.
16. Zhang, Y.; Rundell, A. IEE Proc Syst Biol 2006,153, 201–211.
17. Emery, A. F.; Nenarokomov, A. V. Meas Sci Technol 1998, 9, 864–876.
18. Faller, D.; Klingmuller, U.; Timmer, J. Simulation 2003, 79, 717–725.
19. Gadkar, K. G.; Gunawan, R.; Doyle, F. J., III. BMC Bioinf 2005, 6(155), 151–120.
20. Rodriguez-Fernandez, M.; Mendes, P.; Banga, J. R. BioSystems 2006, 83, 248–265.
21. Zak, D. E.; Gonye, G. E.; Schwaber, J. S.; Doyle, F. J., III. Genome Res 2003, 13, 2396–2405.
22. Gadkar, K. G.; Varner, J.; Doyle, F. J., III. IEE Proc Syst Biol 2005, 2, 17–30.
23. Kutalik, Z.; Cho, K.-H.; Wolkenhauer, O. BioSystems 2004, 75, 43–55.
24. Banga, J. R.; Versyck, K. J.; Van Impe, J. F. Ind Eng Chem Res 2002, 41, 2425–2430.
25. Kell, D. B. Febs J 2006, 273, 873–894.
26. Kruse, K.; Elf, J. In System Modeling in Cellular Biology: From Concepts to Nuts and Bolts; Szallasi, Z.; Stelling, J.; Periwal, V. (Eds.); MIT Press: Cambridge, MA, 2006.
27. Rao, C. V.; Wolf, D. M.; Arkin, A. P. Nature 2002, 420, 231–237.
28. Hoffmann, A.; Levchenko, A.; Scott, M. L.; Baltimore, D. Science 2002, 298, 1241–1245.
29. Nelson, D. E.; Ihekwaba, A. E. C.; Elliott, M.; Johnson, J. R.; Gibney, C. A.; Foreman, B. E.; Nelson, G.; See, V.; Horton, C. A.; Spiller, D. G.; Edwards, S. W.; McDowell, H. P.; Unitt, J. F.; Sullivan, E.; Grimley, R. L.; Benson, N.; Broomhead, D. S.; Kell, D. B.; White, M. R. H. Science 2004, 306, 704–708.

30. Lipniacki, T.; Paszek, P.; Brasier, A. R.; Luxon, B.; Kimmel, M. J Theor Biol 2004, 228, 195–215.
31. Ihekwaba, A. E. C.; Broomhead, D. S.; Grimley, R. L.; Benson, N.; Kell, D. B. IEE Proc Syst Biol 2004, 1, 93–103.
32. Ihekwaba, A. E. C.; Broomhead, D. S.; Grimley, R. L.; Benson, N.; White, M. R. H.; Kell, D. B. IEE Proc Syst Biol 2005, 152, 153–160.
33. Yue, H.; Brown, M.; Knowles, J.; Wang, H.; Broomhead, D. S.; Kell, D. B. Molec BioSystems 2006, 2, 640–649.
34. Goodwin, G. C. Identification: Experimental Design; Pergamon Press: Oxford, UK, 1987.
35. Atkinson, A. C.; Donev, A. N. Optimum Experimental Design; Oxford Science Publications; New York, 1996.
36. Flaherty, P.; Jordan, M. I.; Arkin, A. P. In Proceedings of the Neural Information Processing Symposium, 2005.
37. Boyd, S.; Vandenberghe, L. Convex Optimization; Cambridge University Press; Cambridge, UK, 2004.
38. Morris, M. D. Technometrics 1991, 33, 161–174.
39. Jin, Y.; Yue, H.; Brown, M.; Liang, Y.; Kell, D. B. In American Control Conference, New York, July 2007; pp 2708–2713.
40. Saltelli, A.; Chan, K.; Scott, E. M. (Eds.). Sensitivity Analysis; Wiley West Sussex, UK, 2000.
41. Sung, M.-H.; Simon, R. Mol Pharmacol 2004, 66, 70–75.
42. Kim, J.; Bates, D. G.; Postlethwaite, I.; Ma, L.; Iglesias, P. A. IEE Proc Syst Biol 2006, 153, 96–104.